

1     **Identifying Abnormal Tank Emissions Using Ethane to Methane Signatures of Oil**  
2                     **and Natural Gas Production in the Permian Basin**

3  
4     **Dana R. Caulton<sup>1</sup>, Priya D. Gurav<sup>1</sup>, Anna. M. Robertson<sup>1</sup>, Kristen Pozsonyi<sup>1</sup>, Shane M.**  
5     **Murphy<sup>1</sup>, David R. Lyon<sup>2</sup>**

6     <sup>1</sup> Department of Atmospheric Science, University of Wyoming, Laramie, WY, USA.

7     <sup>2</sup> Environmental Defense Fund, Austin, TX, USA.

8     Corresponding author: Dana R. Caulton ([dcaulton@uwyo.edu](mailto:dcaulton@uwyo.edu))

9     **Key Points:**

- 10         ● Oil and gas production sites in the Permian Basin had a logarithmic mean ethane to  
11             methane ratio of 18%.
- 12         ● Source specific ethane to methane ratios showed that on average tanks on production  
13             sites had higher ratios at 44%.
- 14         ● Tanks with high ethane to methane ratios had statistically lower methane emissions than  
15             tanks with lower ethane to methane ratios.

17 **Abstract**

18 There has been increasing interest in quantifying methane emissions from a view towards  
19 mitigation. Accordingly, ground-based sampling of oil and gas production sites in the Permian  
20 Basin was carried out in January and October 2020. Ethane to methane ratios (EMRs) were  
21 quantified which may be used to distinguish emissions from particular sources, such as produced  
22 gas and oil tank flashing. The logarithmic mean EMR for 102 observations was 18 ( $\pm 2$ )%, while  
23 source specific EMRs showed that sites where emissions were attributed to a tank produced  
24 much higher EMRs averaging 44%. Sites with other noticeable sources such as compressors,  
25 pneumatics, and separators had lower and less variable EMRs. Tanks displayed distinct behavior  
26 with EMRs between 10-21% producing CH<sub>4</sub> emissions >30x higher than tanks with EMRs  
27 >21%. This observation supports the hypothesis that high emission rate tank sources are often  
28 caused by separator malfunctions that leak produced gas through liquids storage tanks.

29

30 **Plain Language Summary**

31 There has been increasing interest in quantifying methane emissions from a view towards  
32 mitigation. One sector of particular interest is oil and gas. To that end, a sampling campaign was  
33 deployed in the Permian Basin, one of the largest oil and gas production sites in the US that has  
34 seen an increase in the production of associated gas since 2006. We quantified the ratio of ethane  
35 co-emitted with methane and found that this ratio showed variability associated with the different  
36 production sources on site. One source (oil and condensate tanks) had an elevated ratio, relative  
37 to other noticeable sources. Tanks also displayed behavior where higher ratios were associated  
38 with lower methane emissions. This suggests that methane emissions from tanks are a result of  
39 abnormal conditions (such as separator malfunctions that leak produced gas through liquids  
40 storage tanks) and ethane to methane ratios may be used to identify such tanks.

41

## 42 **1. Introduction**

43           There has been considerable increase in oil and natural gas (ONG) production in the U.S.  
44 in the past decade that creates the possibility of an increase in associated methane ( $\text{CH}_4$ )  
45 emissions, which numerous studies have noted (Alvarez et al., 2018; Franco et al., 2016;  
46 Hausmann et al., 2016; Helmig et al., 2016; Nisbet et al., 2019; Raimi, 2019; Schneising et al.,  
47 2014). The Permian Basin in Texas and New Mexico covers more than 75,000 square miles  
48 (EIA, 2020). It is the largest oil producing shale formation in the US with 5,208 thousand  
49 barrels/day of oil and 20,280 million cubic feet per/day of NG as of April 2022 (EIA, 2022).  
50 Hence, there has been interest to quantify and mitigate the  $\text{CH}_4$  emissions from this region. A  
51 recent ground-based study reported well-pad  $\text{CH}_4$  emissions in the Permian 5-9 times higher than  
52 EPA inventory estimates (Robertson et al., 2020). Airborne and satellite analysis has also  
53 produced  $\text{CH}_4$  emission rates that are also higher the inventory estimates (Chen et al., 2022;  
54 Irakulis-Loitxate et al., 2021; Schneising et al., 2020; Zhang et al., 2020). Recent work to  
55 constrain total  $\text{CH}_4$  emissions from the Permian Basin have reported emissions from the  
56 production sector contributing ~50% of the total basin emissions (Chen et al., 2022; Cusworth et  
57 al., 2021). These studies also suggest that the largest emissions are well above the emission range  
58 seen from ground campaigns but could not distinguish the on-site source of emissions in most  
59 cases, though intermittent flares were identified as contributing 12% of emissions (Cusworth et  
60 al., 2021). Ground-based samples require large sample sizes to catch these ‘super-emitters’,  
61 which are infrequent and/or short-lived and have a low probability of being randomly sampled  
62 (Wang et al., 2022). Additionally, sources with lofted plumes (such as flares) may be impossible  
63 to quantify via ground-based methods if the plume remains above the measurement height.

64           The production sector includes well pads and tank batteries where a typical ONG well  
65 pad may consist of oil derricks or wellheads, compressors, crude or condensate tanks, produced  
66 water tanks, pneumatic controllers, and flaring units (EIA, 2021). Some of the routine activities  
67 like venting, use of pneumatic controllers, unintentional leakages, malfunctioning flaring units,  
68 and storage tanks contribute to the overall emissions from the production sector (Allen et al.,  
69 2022, 2015a, 2015b; Tyner & Johnson, 2021; Zimmerle et al., 2022). One method to identify a  
70 specific  $\text{CH}_4$  source is by measuring a tracer gas emitted along with  $\text{CH}_4$  such as ethane ( $\text{C}_2\text{H}_6$ ).  
71  $\text{C}_2\text{H}_6$  is primarily emitted from ONG sources and thus has been used as a suitable tracer to

72 distinguish ONG emissions from other sources such as livestock (Peischl et al., 2018; Pollack et  
73 al., 2022; Smith et al., 2015).

74 Previous work has provided limited differentiated ethane to methane ratios (EMRs) for  
75 specific sources of various types of fossil fuel extraction and refining (Yacovitch et al., 2014,  
76 2017, 2020). More commonly, EMRs are reported for large areas. Kort et al., (2016) determined  
77 the C<sub>2</sub>H<sub>6</sub> emissions and the EMR from the Bakken shale region in North Dakota using aircraft  
78 measurements. Similarly, using airborne CH<sub>4</sub> and C<sub>2</sub>H<sub>6</sub> measurements, Smith et al., (2015)  
79 determined EMRs for the microbial, low C<sub>2</sub>H<sub>6</sub> fossil, and high C<sub>2</sub>H<sub>6</sub> fossil sources in the Barnett  
80 Shale region in Texas. Peischl et al., (2018) characterized CH<sub>4</sub> and C<sub>2</sub>H<sub>6</sub> fluxes for several ONG  
81 regions around the U.S. Both Peischl et al., (2018) and Smith et al., (2015) were able to quantify  
82 ONG CH<sub>4</sub> emissions in regions of mixed sources and demonstrate the use of these EMRs in  
83 constraining their results. More recently, estimates of EMRs for different oil-bearing and dry gas  
84 regions were used to identify the importance of oil reservoirs (like the Permian) as dominant  
85 sources of CH<sub>4</sub> among ONG activities (Tribby et al., 2022).

86 EMRs for specific ONG processes may be expected to change with geology, which  
87 affects the initial gas composition and can be quite variable (Tzompa-Sosa et al., 2017).  
88 Downstream of the production sector, the EMR of gas is lowered as ethane and other natural gas  
89 liquids are separated and the processed gas (>95% CH<sub>4</sub>) is sent via the transmission sector to  
90 customers (API, 2021). Flaring may lower the EMR from the source gas as ethane is expected to  
91 combust more efficiently than methane, but this will depend on meteorology, gas exit velocity,  
92 and flame stability (API, 2021; Leahey et al., 2001). At many sites, produced water, condensate,  
93 and oil containing dissolved gases are stored on site in tanks at near-atmospheric pressure after  
94 being passed through a high-pressure separator that separates natural gas from liquids. The tanks  
95 periodically vent as pressure exceeds a set point, causing a quick release of the dissolved gas.  
96 These emissions are known as tank ‘flashing’ and the EMR will be a function of the dissolved  
97 gas concentrations and each species’ solubility, which is affected by temperature and pressure  
98 (API, 2021); crude and condensate tank flashing typically has higher EMRs than the associated  
99 produced gas (Cardoso-Saldana et al., 2021). This study focuses on the use of ethane as a tracer  
100 to differentiate sources within the production sector in the Permian Basin. We measured C<sub>2</sub>H<sub>6</sub>  
101 concentrations simultaneously with CH<sub>4</sub> and calculated site specific EMRs that were then  
102 assigned to the identified emitting sources on site.

## 103 **2. Methods and Data processing**

104 Using the University of Wyoming mobile lab (Robertson et al., 2017), two sampling  
105 campaigns were completed in January 2020 and October-November 2020. ONG sites in the  
106 Permian Basin in Texas and New Mexico were sampled. The region sampled primarily covered  
107 the Delaware Basin, which is the western portion of the Permian Basin. A map of the sampled  
108 locations is provided in Figure S2.

### 109 2.1. Data Collection

110 The University of Wyoming mobile lab included a 2D weather station, 3D sonic  
111 anemometer, and an inlet mounted 4 m above the ground connected to a gas sampling manifold.  
112 Inside the van, a 2Hz Picarro Cavity Ring-Down Spectrometer (CRDS, Model G2204) was used  
113 to measure CH<sub>4</sub> by sampling from the manifold. C<sub>2</sub>H<sub>6</sub> measurements were also collected from  
114 the manifold using an Aerodyne Ethane-Mini spectrometer, a tunable infrared laser direct  
115 absorption spectroscopy instrument (QC-TILDAS), which has a frequency of 1 Hz (Yacovitch et  
116 al., 2014). The Picarro CRDS was calibrated using a high-precision standard CH<sub>4</sub>/C<sub>2</sub>H<sub>6</sub> air mixture  
117 created by the WMO/GAW Central Calibration Laboratories at NOAA's Global Monitoring  
118 Division with  $1936.3 \pm 0.2$  ppb CH<sub>4</sub> and  $2.09 \pm 0.01$  ppb C<sub>2</sub>H<sub>6</sub>. This was carried out twice  
119 throughout the sampling campaign. The reported precision for the CH<sub>4</sub> measurements was 2 ppb  
120 in 5s and the reading was always within 2.5 ppb of the standard. Similarly, for the calibration of  
121 Aerodyne Ethane-Mini spectrometer, the CH<sub>4</sub>/C<sub>2</sub>H<sub>6</sub> air mixture was used and the instrument was  
122 zeroed every 30 minutes using ultra high-purity zero air. The calculated precision for the C<sub>2</sub>H<sub>6</sub>  
123 measurements was 80 ppt in 1s and the reading was always within 0.3 ppb of the standard.

124 As part of the Environmental Defense Fund's Permian Methane Analysis Project  
125 (PermianMAP), this campaign was designed to capture data suitable for CH<sub>4</sub> emission  
126 calculations using OTM 33A (Brantley et al., 2014; US-EPA 2014, 2014). Accordingly, OTM  
127 33A data was collected while the van was stationary and downwind of a source for at least 20  
128 mins. Optical gas imaging using a FLIR camera (model GF300) was taken during sampling and  
129 whenever possible the source of emissions was noted. Occasionally during this campaign  
130 transects were driven downwind of sources suitable for emission calculation by transect method  
131 (Caulton et al., 2018). The OTM 33A and transect data were used to calculate EMRs, which is  
132 the focus of this work.

## 2.2. Data Processing

Ratios were calculated by least squares regression between the CH<sub>4</sub> and C<sub>2</sub>H<sub>6</sub> mixing ratios where the slope of the fit represents the EMR. The reported 95% confidence interval (CI) for each ratio is calculated from the uncertainty of the slope. These ratios are expressed as a percentage of the CH<sub>4</sub> mixing ratio (ppb/ppb × 100). Ratios were screened to remove sites that showed low correlation (R<sup>2</sup> value) between C<sub>2</sub>H<sub>6</sub> and CH<sub>4</sub>. The R<sup>2</sup> value used to screen out sites was 0.65 (Yacovitch et al., 2014).

## 3. Results and Discussion

### 3.1. Sites with Multiple EMR Signatures

A few sites sampled (n=12) displayed two distinct EMR signals (Figure S1). Many of these sites were initially screened out due to low correlation coefficients stemming from the fact that a single fit could not represent the data. The EMR signatures can also be used to parse the total CH<sub>4</sub> flux from the site into the contributions from individual signals, as detailed in the Supplemental Information (SI). This calculation requires the total site CH<sub>4</sub> and C<sub>2</sub>H<sub>6</sub> emissions calculated either via OTM 33A or transect method and individual EMRs. Not all sites produced two signals that passed the R<sup>2</sup> screening threshold and thus not all sites could be parsed. Analysis of the wind direction data was used to identify the probable sources based on site notes and photographs when possible. Results for this analysis are presented in Tables S1-S2. In general, the few sites with multiple EMR signatures where one signal could be attributed to a tank showed that non-tank sources typically were the largest CH<sub>4</sub> source. Further discussion of tanks with respect to EMRs and CH<sub>4</sub> emission overall is presented in Section 3.2.

As an example of this process, we discuss Sites S02 and S03 measured on 22 Jan. 2020 in more detail. These were repeat measurements of the same site and present a unique case study. Prior to sampling, FLIR videos identified that the emissions coming from a separator and a tank, which were about 65 m apart on the site. Pre-measurement transects showed consistent distinct peaks for these sources (Figure S3). The initial sampling was oriented in the centerline of the separator plume, and it was observed that the emission from the tank on site would not be fully captured. The initial OTM 33A measurement (S02) was completed, and afterward the team moved position to the centerline of the tank plume and completed another measurement (S03).

162 The low EMR is remarkably consistent between these sites (3.3% for S02 and 3.5% for S03).  
163 However, in S03 there is an additional signal observable in the data that returns an EMR of 21%  
164 coming from a tank. Additional analysis to corroborate the source signals and contributions are  
165 provided in the SI, which included using the transect plumes to calculate component emissions.  
166 Using the parsing method, the contribution of the total CH<sub>4</sub> emission from the tank to the S03  
167 emission is small (7% of the total emission) and reasonably consistent with source specific  
168 emission estimates calculated from the transects (13% of the total emission).

169 This analysis of separate signals increased our sample size of screened EMRs from 88 to  
170 102 and is used for the remainder of the analysis. These EMRs correspond to a unique site, or to  
171 a unique component on a site. There are at most two EMRs per site. The range of ratios  
172 calculated varied from 3.3% to 157%. Statistics of this dataset are reported using bootstrapping  
173 of 1000 samples with replacement. The mean and median ratios with 95% CIs were 26 ( $\pm 6$ )%  
174 and 14 ( $\pm 1$ )%, respectively. In addition, the logarithmic mean was calculated as 18 ( $\pm 2$ )%. More  
175 than 50% of the observations had EMRs between 10-20%, which likely represents produced gas;  
176 however, we observed several ratios over 100% indicative of oil or condensate tank flashing. The  
177 distribution of EMRs displays right hand skewness (skew = 2.8). Figure S4 shows the  
178 distribution of EMRs on normal and lognormal axes.

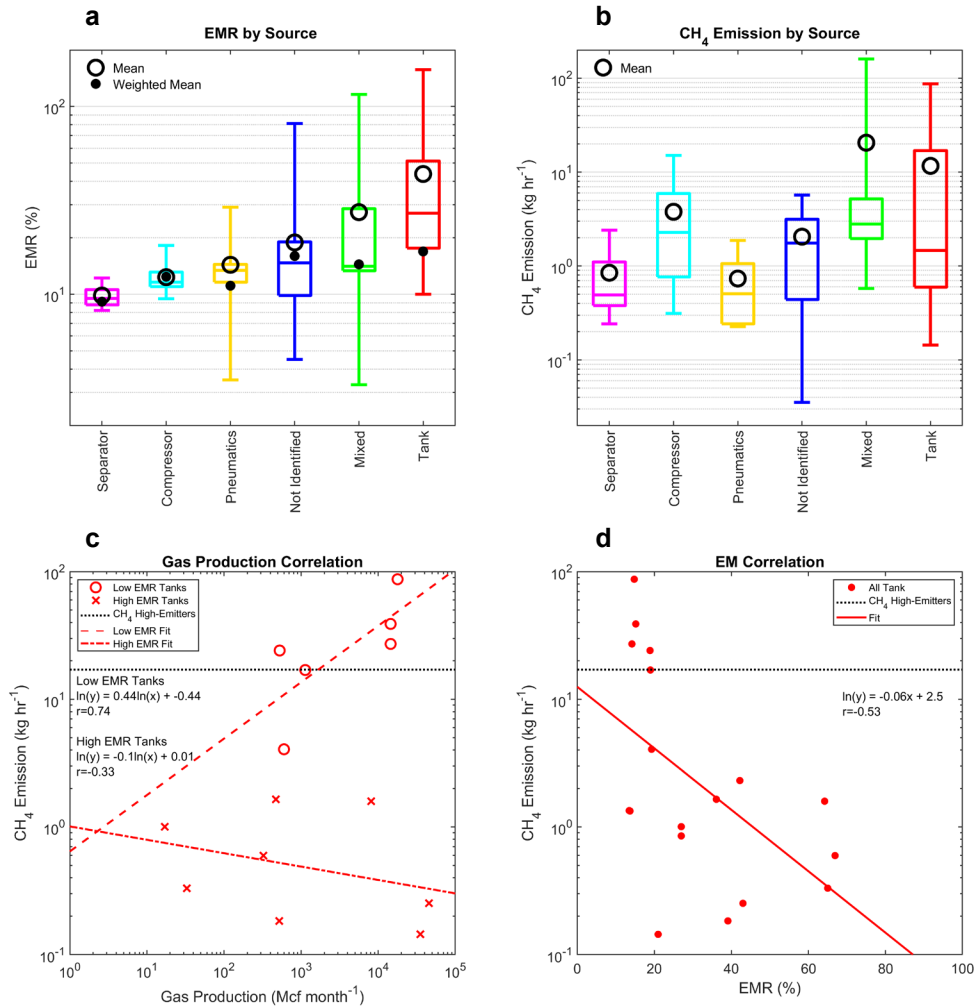
### 179 3.2. Source Specific EMR Signatures

180 Sites were never sampled when operator activity was observed, thus no sources should  
181 represent maintenance activity or manual liquid unloadings. Bell et al., (2017) observed that  
182 OTM 33A underestimated sites from manual liquid unloadings, which contributed significant  
183 fractions of the total emissions in their sample. Though Bell et al., (2017) also noted  
184 underestimation of emissions from OTM 33A more recent work using controlled releases from a  
185 variety of well pad infrastructure generally showed good agreement, however, their release rates  
186 did not span above 2.15 kg hr<sup>-1</sup> (Eddie et al., 2020). Thus, we assume that the emissions estimates  
187 for these sites are robust and do not primarily contain sources that would have lofted plumes the  
188 ground sampling technique could not measure accurately. Sites were grouped by common source  
189 emission type for analysis of differences in EMRs. As sites can have multiple sources this  
190 analysis is not without some subjectivity, and it is possible that the identified source was not the  
191 only or primary source at a site. However, this procedure is consistent with the general way leaks

192 are detected via optical gas imaging (for example in Bell et al., (2017)) albeit without on-site  
193 access. The team made observations by FLIR camera as close to the sources as possible from  
194 publicly accessible land (typically at the edge of the well pad or road). The source categories  
195 defined for this analysis included ‘compressor’, ‘pneumatics’, ‘separator’, and ‘tank’. A source  
196 category contained any emission relating to that source type (e.g., tanks include any type of vent,  
197 pipe or thief hatch on a tank and any type of tank: oil, condensate, produced water, saltwater).  
198 Any site with more than one source noted was put into a ‘mixed signal’ category. Additionally,  
199 some sites had no obvious source, or no information recorded at the time of sampling, and were  
200 grouped together as ‘none/not identifiable’. Full details of the source observations from each site  
201 are reported in Table S3. The results of this analysis are shown in Figure 2 with statistics  
202 reported in Table S4.

203

204



205 **Figure 2.** Box plots showing results of all sampled sites for (a) the EMR and (b) the CH<sub>4</sub>  
 206 emission by source type. Box plots show the 25<sup>th</sup>, 50<sup>th</sup>, and 75<sup>th</sup> percentiles with the minimum  
 207 and maximum data represented by the capped lines (no data is excluded as an outlier). In panel  
 208 (a) the mean is shown an open black dot and the emission weighted mean (Eq. 1) as a filled black  
 209 dot. Panel (c) shows the regression between CH<sub>4</sub> emission and monthly gas production for tank  
 210 sites with low and high EMRs. The delineation of HEs is shown as the dotted black line. Panel  
 211 (d) shows the regression plot between EMR and CH<sub>4</sub> emissions for tank sources along with the  
 212 fit for the data in the solid red line.

213

214 There is a clear increase in average EMR for sites that have only tank emissions. This is  
 215 consistent with observations that have reported high EMRs from tanks and processing equipment  
 216 of wet-gas regions (Goetz et al., 2015, 2017; Yacovitch et al., 2014). In addition, data has shown

217 enhancement of alkane emissions from tank venting and flashing, through modeling and  
 218 measurements (Cardoso-Saldana et al., 2021; Pétron et al., 2012). Mixed signals also show an  
 219 elevated mean EMR. Most of the sites with mixed signals included at least one tank source so it  
 220 is reasonable to assume that the mixed signal EMR is enhanced from the presence of tanks.  
 221 These source categories also showed a large range in EMRs as seen from their large standard  
 222 errors (Table S4). Comparatively, compressors, separators, and pneumatics had relatively  
 223 consistent and lower EMRs. The sites with no identified source information also showed  
 224 elevated EMR signals and higher variability, like the mixed signal category. Though there is a  
 225 broad range of EMRs in the sample, most (>70%) of the sites had ratios <21%. For the 30  
 226 observations with EMRs  $\geq 21\%$ , 17 were directly attributed to tanks, six to sites with mixed  
 227 signals where tanks were present, two to pneumatics, and five were not identifiable. All six sites  
 228 with EMRs over 100% came from tanks or mixed signals where tanks were present. We also  
 229 sampled a ground/pipeline leak (EMR = 13.7%) and an isolated flare emission (EMR = 16.3%).

230 Generally, sites with sources identified as tanks or mixed signals also had higher CH<sub>4</sub>  
 231 emissions, but the range of CH<sub>4</sub> emission observations is larger than the range of EMRs. Also  
 232 shown in Figure 2 and reported in Table S4 are emission weighted mean EMRs. This is  
 233 calculated by multiplying the EMR in a source category by that site's CH<sub>4</sub> emission divided by  
 234 the total CH<sub>4</sub> emissions from that category and summing the individual contributions, as shown  
 235 in Eq. 1:

$$236 \quad \text{Weighted Mean EMR} = \sum_{i=1}^n \text{EMR}(i) \times \frac{\text{CH}_4(i)}{\text{CH}_4 \text{ Total}} \quad \text{Eq. 1}$$

237 Some source categories show consistency between the mean and weighted mean EMR  
 238 including compressors, pneumatics, separators, and even the category where sources were not  
 239 identifiable. Mixed signals and tanks, however, show the largest difference between the mean  
 240 and weighted mean. Tanks in particular have a very high mean (44%) and comparatively low  
 241 weighted mean (17%). This suggests that while high EMRs indicate the presence of a tank, the  
 242 tanks that cause high emissions do not have high EMRs. For the purpose of this analysis, we  
 243 have defined 'high-emitters' (HEs) as sites with a CH<sub>4</sub> emission  $10 \times$  the logarithmic mean of the  
 244 CH<sub>4</sub> emissions of this dataset (HE > 17 kg hr<sup>-1</sup>). This value is not meant to be a universal  
 245 standard, and all but one of the sites measured had CH<sub>4</sub> emission rates < 100 kg hr<sup>-1</sup>. This  
 246 procedure identified seven sites or ~10% of the dataset of CH<sub>4</sub> emissions as HEs. For tanks with  
 247 EMR values  $\geq 21\%$ , none of the emissions can be classified as HEs. All the tanks associated with

248 HEs in this data set had EMRs between 10-21%. The mean CH<sub>4</sub> emission rate for these low  
249 EMR tanks (n=8) was over 30 times higher and statistically different from than the mean CH<sub>4</sub>  
250 emission rate for tanks with high EMRs (n=12). Statistics for the tanks broken up by EMR are  
251 reported in Table S5.

252 To explain these observations, we theorize that the high EMRs represent normal tank  
253 operations (e.g., flashing, working, and standing losses) that do not appear to be primarily  
254 associated with high emissions. Rather, the high CH<sub>4</sub> emissions may occur during abnormal  
255 conditions where separator or other issues pass unprocessed gas directly to the tank where it can  
256 leak to the atmosphere. This hypothesis is supported by other work that has suggested emissions  
257 from ONG primarily arise from abnormal conditions (Alvarez et al., 2018; Luck et al., 2019;  
258 Daniel Zavala-Araiza et al., 2017). The precise source of the abnormal condition may be similar  
259 or related to a known emission point from separator dump valves, which are used to release  
260 accumulated liquids and can become stuck open due to debris or other issues (API, 2021).

261 There is little direct support for this theory without on-site reports of equipment status. In  
262 the absence of such data, we have looked at site characteristics for further evidence. Not all of  
263 the low EMR tanks produced large CH<sub>4</sub> emissions. If these low EMR tanks primarily represent  
264 abnormal conditions, one factor limiting the amount of CH<sub>4</sub> that can be emitted is the amount of  
265 produced gas. Generally, there has been little evidence for significant relationships between gas  
266 production and site-level CH<sub>4</sub> emissions and we assume that most sites in these studies were  
267 operating normally; thus for normally operating sites we expect a moderate to weak relationship  
268 between these parameters (Brantley et al., 2014; Lyon et al., 2016; Omara et al., 2016; D.  
269 Zavala-Araiza et al., 2018). We separated the tanks by low and high EMR and regressed them  
270 against the gas production corresponding to the month of measurement to investigate the  
271 significance of these relationships. The results of this analysis are shown in Figure 2. Low EMR  
272 tanks showed a positive correlation ( $r = 0.74$ ) between the natural log of monthly gas production  
273 and CH<sub>4</sub> emissions. However, the slope of this fit is not statistically different from 0. On the  
274 other hand, the regression between the natural log of monthly gas production and CH<sub>4</sub> emissions  
275 for high EMR tanks shows weak negative correlation ( $r = -0.33$ ). For reference, the entire data set  
276 showed weak correlation between these parameters ( $r = 0.11$ ). Following this analysis, the  
277 identification of HEs from tanks from this data set is consistently predicted by the presence of a

278 low EMR and high gas production value. More observations are needed to corroborate this  
279 theory, particularly with sites with even higher CH<sub>4</sub> emission rates (>100 kg hr<sup>-1</sup>).

280 We caution that as subcategories are further divided, the number of observations in any  
281 category becomes increasingly small and prone to spurious relationships. It should also be noted  
282 that there is no evidence for a direct correlation between EMR and CH<sub>4</sub> emissions. Using a  
283 regression of the calculated ratios versus the calculated OTM 33A or transect CH<sub>4</sub> emissions  
284 (n=65), we found a Pearson correlation coefficient of -0.1. The correlation is only statistically  
285 significant (p<0.05) for tanks with a correlation coefficient of -0.53 (Figure 2). However, there  
286 appears to be two distinct regions to the tanks EMR vs CH<sub>4</sub> correlation corresponding to the 21%  
287 EMR threshold previously identified. Complicating this analysis is the fact that the CH<sub>4</sub>  
288 distribution of this dataset is more positively skewed (skew = 5.1) than the EMR distribution  
289 (skew = 2.8). This is consistent with observations of CH<sub>4</sub> emissions from ONG operations that  
290 show extreme right skew behavior, which has been observed in the Permian as well (Brandt et  
291 al., 2016; Robertson et al., 2020). The presence of HEs that occur at low frequency has the effect  
292 of substantially altering the mean of any data set. Therefore, it is appropriate to use caution when  
293 interpreting trends associated with these extremes. The conclusion that tanks have statistically  
294 higher mean EMRs than any other identified source is robust and consistent with previous  
295 observations (Cardoso-Saldana et al., 2021; Goetz et al., 2015, 2017). The observation that tanks  
296 with low EMRs have on average higher CH<sub>4</sub> emissions than tanks with high EMRs is also  
297 statistically robust, and a novel finding of this work. The interpretation that there is a direct  
298 relationship between gas production and CH<sub>4</sub> emission for low EMR tanks, and an inverse  
299 relationship between EMR and CH<sub>4</sub> emission from tanks requires more observations to  
300 corroborate because HEs occur infrequently and can dramatically alter the regressions.

### 301 3.3. Regional EMR

302 As mentioned, the range of EMRs observed in this data produced a skewed distribution.  
303 This distribution yielded a range of statistics with different values, as stated earlier, with a mean,  
304 median and logarithmic mean of 26 (±6)%, 14 (±1)%, and 18 (±2)%, respectively. This gives rise  
305 to the question of which statistic is most appropriate for comparison to other literature or useful  
306 for other analysis. Because the uncertainty on most of the statistics was relatively high, we also  
307 calculated a regional EMR through regression analysis of the background concentration data

308 collected when transiting between sites. For this analysis, background data was calculated as a  
309 running mean of the lowest 30% of the data in 30s bins, which removed sharp peaks, but  
310 preserved large scale variations in the background. Some results of this procedure are show in  
311 Figure S5. The background data was then regressed to produce an EMR that should be  
312 representative of the weighted EMR for the region including sectors other than production.  
313 However, because this area was dominated by production sites, the ratio is expected to be similar  
314 to the production sector. We also separated the data based on the season of measurement to  
315 observe temporal trends in the EMR. The EMR ranged from 16.77 ( $\pm 0.02$ )% in winter to 18.98  
316 ( $\pm 0.03$ )% the following fall with a combined ratio of 17.3 ( $\pm 0.2$ )% (Figure S6). There is some  
317 overlap in the sampling area between the winter and fall campaigns though the area is not exactly  
318 the same (Figure S2). The logarithmic mean of the production sector EMRs (18%) compares best  
319 with the regression EMR for the region and may be the best statistic to represent skewed EMR  
320 distributions.

321 An additional vector of comparison can be made using available gas composition data.  
322 (Kort et al., 2016) found that their EMR was consistent with the composition of NG production  
323 data from 710 sites in the Bakken Shale which had an EMR of 42%. Peischl et al., (2018) also  
324 reported C<sub>2</sub>H<sub>6</sub> and CH<sub>4</sub> fluxes for several regions and compared to available gas composition  
325 data in those regions and generally found good agreement. This previous work suggests that gas  
326 composition may be used as a proxy for expected EMRs from production sites. For this study,  
327 we compared our results to the gas composition statistics from 19 wells in the Permian Basin  
328 (ERG, 2012; Fairhurst & Hanson, 2012; Howard et al., 2015). The bootstrapped statistics for the gas  
329 composition mean and median EMR are 13 ( $\pm 3$ )% and 15 ( $\pm 6$ )%, respectively. The gas  
330 composition mean EMR is statistically lower than the mean ratio calculated from this study of  
331 26%. It is also slightly lower (and statistically different) than the regional EMR (17.3%) and  
332 logarithmic mean (18%). The median gas composition EMR is more uncertain, but compares  
333 better with the site EMR statistics and regional EMR calculated in this study. The gas  
334 composition data used in this analysis primarily came from wells in Texas in both the Delaware  
335 and Midland basins, which span a wide geographical area and include areas outside of our study  
336 region (Figure S2). Large datasets of gas composition are not always readily available (as in this  
337 case) and composition varies from well to well, thus comparison to a few wells is not very  
338 meaningful. The gas composition EMR from the available data varied from <1% to 24% and was

339 not normally distributed. In addition, the results presented here show that the surface source  
340 types do not have uniform EMRs suggesting it is more appropriate to actually measure EMRs  
341 than assume gas composition is an equivalent metric.

#### 342 **4. Implications**

343 This study presented calculations of EMRs from 102 screened observations. We observed  
344 a logarithmic mean ratio of 18 ( $\pm 2$ )% for these production sites measured in the Permian basin  
345 that compares well to a regional EMR of 17.3 ( $\pm 0.2$ )%. Component specific EMRs were  
346 calculated with tanks producing the highest average EMR at 44%. Tanks also displayed distinct  
347 behavior in CH<sub>4</sub> emissions for sites that were close to the regional EMR (10-21%) and sites that  
348 had elevated EMRs (21-157%). The highest CH<sub>4</sub> emissions from tanks in this dataset had lower  
349 EMRs and high gas production values. Of the five highest emitting sites in this study, which  
350 contributed 75% of emissions, four sites were categorized as tanks and one as a mixed signal.  
351 However, none of these sites had EMRs over 21%. The observation that tanks are a primary  
352 source of elevated CH<sub>4</sub> emission rates in this dataset is consistent with recent observations that  
353 also identify tanks as a major source of CH<sub>4</sub> emissions (Tyner & Johnson, 2021).

354 We have put forth a hypothesis for these observations which implies that the elevated  
355 CH<sub>4</sub> emissions from tanks are mainly from produced gas escaping through the tank, rather than  
356 tank flashing. This indicates these high tank CH<sub>4</sub> emissions are driven by abnormal conditions  
357 and perhaps caused by or related to separator issues such as a stuck dump valve. Therefore,  
358 EMRs could have use for determining when detected emissions are normal vs abnormal. EMRs  
359 are computationally easy as they can be calculated directly from concentration measurements  
360 and do not rely on meteorology. We used ~20 minutes of data for these calculations, but we were  
361 also able to calculate EMRs from aborted OTM 33A measurements and transects that lasted only  
362 a few minutes. It may be possible to quickly quantify the EMR from tanks to determine whether  
363 they are behaving abnormally and implement remediation, regardless of gas production value.  
364 Gas production value may have use for optimizing such a strategy to target high CH<sub>4</sub> emission  
365 sites.

366 In addition to distinguishing production sources, EMRs may have use in defining the  
367 contribution of sector emissions at large scales. Though previous work has shown that the mean  
368 EMR is generally close to the gas composition of the region (Kort et al., 2016; Peischl et al.,

369 2015, 2018), this work showed that EMRs varied by source, suggesting raw gas composition  
370 data is not an accurate representation of the surface emission EMRs, especially in areas that have  
371 equipment such as tanks (i.e., wet gas/associated gas regions). Other recent work has made an  
372 argument against using gas composition in regions where transmission sector equipment  
373 produces lower EMRs than expected by gas composition data (Zimmerle et al., 2022). In  
374 addition, measurements of processing equipment have shown a range of EMRs and even  
375 scenarios where C<sub>2</sub>H<sub>6</sub> is released without CH<sub>4</sub> (Roscioli et al., 2015; Yacovitch et al., 2014,  
376 2015). This illustrates the likely variability of EMR signatures across sectors in addition to  
377 regional differences. Cusworth et al., (2021) estimated the distribution of emissions based on  
378 sector in the Permian in 2019. It may be possible to corroborate such contributions from different  
379 sectors using C<sub>2</sub>H<sub>6</sub> observations if they are associated with different mean EMRs. As Smith et  
380 al., (2015) showed, there is considerable uncertainty when attempting to use only C<sub>2</sub>H<sub>6</sub> and CH<sub>4</sub>  
381 to partition signals in a region with multiple EMRs. Observations of other tracers, like CO<sub>2</sub> or  
382 H<sub>2</sub>S may be necessary to fully implement such analysis.

383 Finally, the results presented here provide some implications for low-cost sensors, which  
384 have been gaining increasing attention as a cheap and large-scale monitoring solution (Riddick et  
385 al., 2022; Zhou et al., 2021). Because most low-cost sensors like photoionization detectors  
386 (PIDs) are not very selective, they may be prone to producing false high emission rates when  
387 they are in the plume of a tank, due to the presence of interfering hydrocarbons. This could lead  
388 to consistent ‘false positive’ reading for tank emissions and limit the efficiency of leak detection  
389 from PIDs.

## 390 **Acknowledgments**

391 The authors declare no competing financial interests. This work was funded by the  
392 Environmental Defense Fund as part of the Permian Methane Analysis Project (PermianMAP)  
393 campaign. PermianMAP, which includes the aerial, tower, and flare survey data, is grateful for  
394 the support of Bloomberg Philanthropies, Grantham Foundation for the Protection of the  
395 Environment, High Tide Foundation, the John D. and Catherine T. MacArthur Foundation,  
396 Quadrivium, and the Zegar Family Foundation. The School of Energy Resources at the  
397 University of Wyoming also provided financial support for the mobile lab, instrumentation and  
398 students. We would like to thank Megan McCabe for help in data collection during the January

399 '20 campaign, Matt Burkhart and Zane Little for technical support and maintenance of the  
400 mobile lab and Jack Warren for help in obtaining and aggregating the gas production data from  
401 Enverus.com.

402 CRediT Author Statement

- 403 • D.R.C.: Supervision, Conceptualization, Visualization, Writing-Original Draft
- 404 • P.D.G.: Formal analysis, Data curation, Writing-Reviewing and Editing
- 405 • A.M.R.: Project administration, Formal analysis, Data Curation, Writing-Reviewing  
406 and Editing
- 407 • K.P.: Data Curation
- 408 • S.M.R.: Funding Acquisition, Conceptualization, Writing-Reviewing and Editing
- 409 • D.R.L.: Writing-Reviewing and Editing

410 **Open Research**

411 The data containing EMRs, CH<sub>4</sub> emissions and supporting information will be made available at  
412 <https://data.permianmap.org/>. This data repository is maintained by the Environmental Defense  
413 Fund and is free and open to the public with agreement to abide by the terms of use, which are  
414 available at the website.

415

416

417 **References**

- 418 Allen, D. T., Sullivan, D. W., Zavala-Araiza, D., Pacsi, A. P., Harrison, M., Keen, K., et al.  
419 (2015a). Methane emissions from process equipment at natural gas production sites in the  
420 United States: Liquid unloadings. *Environmental Science and Technology*, 49(1), 641–648.  
421 <https://doi.org/10.1021/es504016r>
- 422 Allen, D. T., Pacsi, A. P., Sullivan, D. W., Zavala-Araiza, D., Harrison, M., Keen, K., et al.  
423 (2015b). Methane emissions from process equipment at natural gas production sites in the  
424 United States: Pneumatic controllers. *Environmental Science and Technology*, 49(1), 633–  
425 640. <https://doi.org/10.1021/es5040156>
- 426 Allen, D. T., Cardoso-Saldaña, F. J., Kimura, Y., Chen, Q., Xiang, Z., Zimmerle, D., et al.  
427 (2022). A Methane Emission Estimation Tool (MEET) for predictions of emissions from  
428 upstream oil and gas well sites with fine scale temporal and spatial resolution: Model  
429 structure and applications. *Science of the Total Environment*, 829.  
430 <https://doi.org/10.1016/j.scitotenv.2022.154277>
- 431 Alvarez, R. A., Zavala-Araiza, D., Lyon, D. R., Allen, D. T., Barkley, Z. R., Brandt, A. R., et al.  
432 (2018). Assessment of methane emissions from the U.S. oil and gas supply chain. *Science*,  
433 361(6398), 186–188. <https://doi.org/10.1126/science.aar7204>
- 434 API. (2021). *COMPENDIUM OF GREENHOUSE GAS EMISSIONS METHODOLOGIES FOR*  
435 *THE NATURAL GAS AND OIL INDUSTRY COMPENDIUM OF GREENHOUSE GAS*  
436 *EMISSIONS METHODOLOGIES FOR THE NATURAL GAS AND OIL INDUSTRY.*
- 437 Bell, C. S., Vaughn, T. L., Zimmerle, D., Herndon, S. C., Yacovitch, T. I., Heath, G. A., et al.  
438 (2017). Comparison of methane emission estimates from multiple measurement techniques  
439 at natural gas production pads. *Elementa Science of the Anthropocene*, 5.  
440 <https://doi.org/10.1525/elementa.266>
- 441 Brandt, A. R., Heath, G. a., & Cooley, D. (2016). Methane Leaks from Natural Gas Systems  
442 Follow Extreme Distributions. *Environmental Science and Technology*, 50(22), 12512–  
443 12520. <https://doi.org/10.1021/acs.est.6b04303>
- 444 Brantley, H. L., Thoma, E. D., Squier, W. C., Guven, B. B., & Lyon, D. (2014). Assessment of  
445 Methane Emissions from Oil and Gas Production Pads using Mobile Measurements.  
446 *Environmental Science and Technology*, 48(24), 14508–14515.  
447 <https://doi.org/10.1021/es503070q>

- 448 Cardoso-Saldana, F. J., Pierce, K., Chen, Q., Kimura, Y., & Allen, D. T. (2021). A searchable  
 449 database for prediction of emission compositions from upstream oil and gas sources.  
 450 *Environmental Science and Technology*, *55*(5), 3210–3218.  
 451 <https://doi.org/10.1021/acs.est.0c05925>
- 452 Caulton, D. R., Li, Q., Bou-Zeid, E., Lu, J., Lane, H. M., Fitts, J. P., et al. (2018). Quantifying  
 453 uncertainties from mobile-laboratory-derived emissions of well pads using inverse Gaussian  
 454 methods. *Atmospheric Chemistry and Physics*, *18*(20), 15145–15168.  
 455 <https://doi.org/10.5194/acp-18-15145-2018>
- 456 Chen, Y., Sherwin, E. D., Berman, E. S. F., Jones, B. B., Gordon, M. P., Wetherley, E. B., et al.  
 457 (2022). Quantifying Regional Methane Emissions in the New Mexico Permian Basin with a  
 458 Comprehensive Aerial Survey. *Environmental Science & Technology*, *56*(7), 4317–4323.  
 459 <https://doi.org/10.1021/acs.est.1c06458>
- 460 Cusworth, D. H., Duren, R. M., Thorpe, A. K., Olson-Duvall, W., Heckler, J., Chapman, J. W.,  
 461 et al. (2021). Intermittency of Large Methane Emitters in the Permian Basin. *Environmental*  
 462 *Science and Technology Letters*, *8*(7), 567–573. <https://doi.org/10.1021/acs.estlett.1c00173>
- 463 Eastern Research Group. (2012). *APPENDIX C: CONDENSATE TANK OIL AND GAS*  
 464 *ACTIVITIES*. Austin, TX.
- 465 Edie, R., Robertson, A. M., Soltis, J., Field, R. A., Snare, D., Burkhart, M. D., & Murphy, S. M.  
 466 (2020). Off-Site Flux Estimates of Volatile Organic Compounds from Oil and Gas  
 467 Production Facilities Using Fast-Response Instrumentation. *Environmental Science and*  
 468 *Technology*, *54*(3), 1385–1394. <https://doi.org/10.1021/acs.est.9b05621>
- 469 EIA. (2020). *Permian Basin Part 2 Wolfcamp Shale Play of the Midland Basin Geology review:*  
 470 *U.S. Energy Information Administration*. Retrieved from  
 471 [https://www.eia.gov/maps/pdf/Permian\\_Wolfcamp\\_Midland\\_EIA\\_reportII.pdf](https://www.eia.gov/maps/pdf/Permian_Wolfcamp_Midland_EIA_reportII.pdf).
- 472 EIA. (2021, December 2). Natural Gas Explained.
- 473 EIA. (2022). *Drilling Productivity Report*. Retrieved from  
 474 <https://www.eia.gov/petroleum/drilling/>
- 475 Fairhurst, B., & Hanson, M. L. (2012). *Evolution and Development of the WolfBone Play,*  
 476 *Southern Delaware Basin, West Texas: An Emerging Frontier, An Oil-Rich Unconventional*  
 477 *Resource #10411*.

- 478 Franco, B., Mahieu, E., Emmons, L. K., Tzompa-Sosa, Z. A., Fischer, E. v., Sudo, K., et al.  
479 (2016). Evaluating ethane and methane emissions associated with the development of oil  
480 and natural gas extraction in North America. *Environmental Research Letters*, 11(4).  
481 <https://doi.org/10.1088/1748-9326/11/4/044010>
- 482 Fritz, B. K., Shaw, B. W., & Parnell, C. B. (2005). INFLUENCE OF METEOROLOGICAL  
483 TIME FRAME AND VARIATION ON HORIZONTAL DISPERSION COEFFICIENTS IN  
484 GAUSSIAN DISPERSION MODELING. *Transactions of the American Society of*  
485 *Agricultural Engineers*, 48(3), 1185–1196. <https://doi.org/10.13031/2013.18501>
- 486 Goetz, J. D., Floerchinger, C., Fortner, E. C., Wormhoudt, J., Massoli, P., Knighton, W. B., et al.  
487 (2015). Atmospheric emission characterization of marcellus shale natural gas development  
488 sites. *Environmental Science and Technology*, 49(11), 7012–7020.  
489 <https://doi.org/10.1021/acs.est.5b00452>
- 490 Goetz, J. D., Avery, A., Werden, B., Floerchinger, C., Fortner, E. C., Wormhoudt, J., et al.  
491 (2017). Analysis of local-scale background concentrations of methane and other gas-phase  
492 species in the Marcellus Shale. *Elementa Science of the Anthropocene*, 5, 1–20.  
493 <https://doi.org/10.1525/elementa.182>
- 494 Hausmann, P., Sussmann, R., & Smale, D. (2016). Contribution of oil and natural gas production  
495 to renewed increase in atmospheric methane (2007-2014): Top-down estimate from ethane  
496 and methane column observations. *Atmospheric Chemistry and Physics*, 16(5), 3227–3244.  
497 <https://doi.org/10.5194/acp-16-3227-2016>
- 498 Helmig, D., Rossabi, S., Hueber, J., Tans, P., Montzka, S. A., Masarie, K., et al. (2016). Reversal  
499 of global atmospheric ethane and propane trends largely due to US oil and natural gas  
500 production. *Nature Geoscience*, 9(7), 490–495. <https://doi.org/10.1038/ngeo2721>
- 501 Howard, T., Ferrara, T. W., & Townsend-Small, A. (2015). Sensor transition failure in the high  
502 flow sampler: Implications for methane emission inventories of natural gas infrastructure.  
503 *Journal of the Air and Waste Management Association*, 65(7), 856–862.  
504 <https://doi.org/10.1080/10962247.2015.1025925>
- 505 Irakulis-Loitxate, I., Guanter, L., Liu, Y.-N., Varon, D. J., Maasackers, J. D., Zhang, Y., et al.  
506 (2021). Satellite-based survey of extreme methane emissions in the Permian basin. *Science*  
507 *Advances*, 7(27), 1–8. <https://doi.org/10.1126/sciadv.abf4507>

- 508 Kort, E. A., Smith, M. L., Murray, L. T., Gvakharia, A., Brandt, A. R., Peischl, J., et al. (2016).  
509 Fugitive emissions from the Bakken shale illustrate role of shale production in global ethane  
510 shift. *Geophysical Research Letters*, *43*(9), 4617–4623.  
511 <https://doi.org/10.1002/2016GL068703>
- 512 Leahey, D. M., Preston, K., & Strosher, M. (2001). Theoretical and observational assessments of  
513 flare efficiencies. *Journal of the Air and Waste Management Association*, *51*(12), 1610–  
514 1616. <https://doi.org/10.1080/10473289.2001.10464390>
- 515 Luck, B., Zimmerle, D., Vaughn, T., Lauderdale, T., Keen, K., Harrison, M., et al. (2019).  
516 Multiday Measurements of Pneumatic Controller Emissions Reveal the Frequency of  
517 Abnormal Emissions Behavior at Natural Gas Gathering Stations. *Environmental Science  
518 and Technology Letters*, *6*(6), 348–352. rapid-communication.  
519 <https://doi.org/10.1021/acs.estlett.9b00158>
- 520 Lyon, D. R., Alvarez, R. A., Zavala-Araiza, D., Brandt, A. R., Jackson, R. B., & Hamburg, S. P.  
521 (2016). Aerial Surveys of Elevated Hydrocarbon Emissions from Oil and Gas Production  
522 Sites. *Environmental Science and Technology*, *50*(9), 4877–4886.  
523 <https://doi.org/10.1021/acs.est.6b00705>
- 524 Nisbet, E. G., Manning, M. R., Dlugokencky, E. J., Fisher, R. E., Lowry, D., Michel, S. E., et al.  
525 (2019). Very Strong Atmospheric Methane Growth in the 4 Years 2014–2017: Implications  
526 for the Paris Agreement. *Global Biogeochemical Cycles*, *33*(3), 318–342.  
527 <https://doi.org/10.1029/2018GB006009>
- 528 Omara, M., Sullivan, M. R., Li, X., Subramian, R., Robinson, A. L., & Presto, A. A. (2016).  
529 Methane Emissions from Conventional and Unconventional Natural Gas Production Sites in  
530 the Marcellus Shale Basin. *Environmental Science and Technology*, *50*(4), 2099–2107.  
531 <https://doi.org/10.1021/acs.est.5b05503>
- 532 Peischl, J., Ryerson, T. B., Aikin, K. C., Gouw, J. A., Gilman, J. B., Holloway, J. S., et al.  
533 (2015). Quantifying atmospheric methane emissions from the Haynesville, Fayetteville, and  
534 northeastern Marcellus shale gas production regions. *Journal of Geophysical Research:  
535 Atmospheres*, (120), 2119–2139. <https://doi.org/10.1002/2014JD022697>
- 536 Peischl, J., Eilerman, S. J., Neuman, J. A., Aikin, K. C., de Gouw, J., Gilman, J. B., et al. (2018).  
537 Quantifying Methane and Ethane Emissions to the Atmosphere From Central and Western

- 538 U.S. Oil and Natural Gas Production Regions. *Journal of Geophysical Research:*  
539 *Atmospheres*, 123(14), 7725–7740. <https://doi.org/10.1029/2018JD028622>
- 540 Pétron, G., Frost, G., Miller, B. R., Hirsch, A. I., Montzka, S. A., Karion, A., et al. (2012).  
541 Hydrocarbon emissions characterization in the Colorado Front Range: A pilot study.  
542 *Journal of Geophysical Research Atmospheres*. Blackwell Publishing Ltd.  
543 <https://doi.org/10.1029/2011JD016360>
- 544 Pollack, I. B., McCabe, M. E., Caulton, D. R., & Fischer, E. v. (2022). Enhancements in  
545 Ammonia and Methane from Agricultural Sources in the Northeastern Colorado Front  
546 Range Using Observations from a Small Research Aircraft. *Environmental Science &*  
547 *Technology*, 56(4), 2236–2247. <https://doi.org/10.1021/acs.est.1c07382>
- 548 Raimi, D. (2019). The Greenhouse Gas Impacts of Increased US Oil and Gas Production.  
549 Washington, DC: Resource for the Future.
- 550 Riddick, S. N., Ancona, R., Cheptonui, F., Bell, C. S., Duggan, A., Bennett, K. E., & Zimmerle,  
551 D. J. (2022). A cautionary report of calculating methane emissions using low-cost fence-  
552 line sensors. *Elementa: Science of the Anthropocene*, 10(1).  
553 <https://doi.org/10.1525/elementa.2022.00021>
- 554 Robertson, A. M., Edie, R., Snare, D., Soltis, J., Field, R. A., Burkhart, M. D., et al. (2017).  
555 Variation in Methane Emission Rates from Well Pads in Four Oil and Gas Basins with  
556 Contrasting Production Volumes and Compositions. *Environmental Science and*  
557 *Technology*, 51(15), 8832–8840. <https://doi.org/10.1021/acs.est.7b00571>
- 558 Robertson, A. M., Edie, R., Field, R. A., Lyon, D., McVay, R., Omara, M., et al. (2020). New  
559 Mexico Permian basin measured well pad methane emissions are a factor of 5–9 times  
560 higher than U.S. EPA estimates. *Environmental Science and Technology*, 54(21), 13926–  
561 13934. <https://doi.org/10.1021/acs.est.0c02927>
- 562 Roscioli, J. R., Yacovitch, T. I., Floerchinger, C., Mitchell, A. L., Tkacik, D. S., Subramanian,  
563 R., et al. (2015). Measurements of methane emissions from natural gas gathering facilities  
564 and processing plants: Measurement methods. *Atmospheric Measurement Techniques*, 8(5),  
565 2017–2035. <https://doi.org/10.5194/amt-8-2017-2015>
- 566 Schneising, O., Burrows, J. P., Dickerson, R. R., Buchwitz, M., Reuter, M., & Bovensmann, H.  
567 (2014). Remote sensing of fugitive methane emissions from oil and gas production in North  
568 American tight geologic formations. *Earth's Future*, 2(10), 548–558.

- 569 Schneising, O., Buchwitz, M., Reuter, M., Vanselow, S., Bovensmann, H., & P. Burrows, J.  
570 (2020). Remote sensing of methane leakage from natural gas and petroleum systems  
571 revisited. *Atmospheric Chemistry and Physics*, 20(15), 9169–9182.  
572 <https://doi.org/10.5194/acp-20-9169-2020>
- 573 Smith, M. L., Kort, E. A., Karion, A., Sweeney, C., Herndon, S. C., & Yacovitch, T. I. (2015).  
574 Airborne Ethane Observations in the Barnett Shale: Quantification of Ethane Flux and  
575 Attribution of Methane Emissions. *Environmental Science and Technology*, 49(13), 8158–  
576 8166. <https://doi.org/10.1021/acs.est.5b00219>
- 577 Tribby, A. L., Bois, J. S., Montzka, S. A., Atlas, E. L., Vimont, I., Lan, X., et al. (2022).  
578 Hydrocarbon Tracers Suggest Methane Emissions from Fossil Sources Occur  
579 Predominately Before Gas Processing and That Petroleum Plays Are a Significant Source.  
580 *Environmental Science & Technology*. <https://doi.org/10.1021/acs.est.2c00927>
- 581 Tyner, D. R., & Johnson, M. R. (2021). Where the Methane Is - Insights from Novel Airborne  
582 LiDAR Measurements Combined with Ground Survey Data. *Environmental Science and*  
583 *Technology*, 55(14), 9773–9783. <https://doi.org/10.1021/acs.est.1c01572>
- 584 Tzompa-Sosa, Z. A., Mahieu, E., Franco, B., Keller, C. A., Turner, A. J., Helmig, D., et al.  
585 (2017). Revisiting global fossil fuel and biofuel emissions of ethane. *Journal of*  
586 *Geophysical Research*, 122(4), 2493–2512. <https://doi.org/10.1002/2016JD025767>
- 587 US-EPA 2014. (2014). *SOP for Analysis of US EPA GMAP-REQ-DA Method Data for*  
588 *Methane Emission Rate Quantification using the Point Source Gaussian Method SOP 601*  
589 *for OTM 33A*.
- 590 Wang, J., Daniels, W. S., Hammerling, D. M., Harrison, M., Burmaster, K., George, F. C., &  
591 Ravikumar, A. P. (2022). Multi-scale Methane Measurements at Oil and Gas Facilities  
592 Reveal Necessary Framework for Improved Emissions Accounting. *EarthArXiv*, 1–37.  
593 <https://doi.org/10.26434/chemrxiv-2022-9zh2v>
- 594 Yacovitch, T. I., Herndon, S. C., Roscioli, J. R., Floerchinger, C., McGovern, R. M., Agnese, M.,  
595 et al. (2014). Demonstration of an ethane spectrometer for methane source identification.  
596 *Environmental Science and Technology*, 48(14), 8028–8034.  
597 <https://doi.org/10.1021/es501475q>
- 598 Yacovitch, T. I., Herndon, S. C., Pétron, G., Kofler, J., Lyon, D., Zahniser, M. S., & Kolb, C. E.  
599 (2015). Mobile Laboratory Observations of Methane Emissions in the Barnett Shale

- 600 Region. *Environmental Science and Technology*, 49(13), 7889–7895.  
601 <https://doi.org/10.1021/es506352j>
- 602 Yacovitch, T. I., Daube, C., Vaughn, T. L., Bell, C. S., Roscioli, J. R., Knighton, W. B., et al.  
603 (2017). Natural gas facility methane emissions: Measurements by tracer flux ratio in two  
604 US natural gas producing basins. *Elementa*, 5(2013). <https://doi.org/10.1525/elementa.251>
- 605 Yacovitch, T. I., Daube, C., & Herndon, S. C. (2020). Methane Emissions from Offshore Oil and  
606 Gas Platforms in the Gulf of Mexico. *Environmental Science and Technology*, 54(6), 3530–  
607 3538. <https://doi.org/10.1021/acs.est.9b07148>
- 608 Zavala-Araiza, D., Herndon, S. C., Roscioli, J. R., Yacovitch, T. I., Johnson, M. R., Tyner, D. R.,  
609 et al. (2018). Methane emissions from oil and gas production sites in Alberta, Canada.  
610 *Elementa: Science of the Anthropocene*, 6(27), 1–13. <https://doi.org/10.1525/elementa.284>
- 611 Zavala-Araiza, Daniel, Alvarez, R. A., Lyon, D. R., Allen, D. T., Marchese, A. J., Zimmerle, D.  
612 J., & Hamburg, S. P. (2017). Super-emitters in natural gas infrastructure are caused by  
613 abnormal process conditions. *Nature Communications*, 8.  
614 <https://doi.org/10.1038/ncomms14012>
- 615 Zhang, Y., Gautam, R., Pandey, S., Omara, M., Maasackers, J. D., Sadavarte, P., et al. (2020).  
616 Quantifying methane emissions from the largest oil-producing basin in the United States  
617 from space. *Science Advances*, 6(17), 1–9. <https://doi.org/10.1126/sciadv.aaz5120>
- 618 Zhou, X., Peng, X., Montazeri, A., McHale, L. E., Gaßner, S., Lyon, D. R., et al. (2021). Mobile  
619 Measurement System for the Rapid and Cost-Effective Surveillance of Methane and  
620 Volatile Organic Compound Emissions from Oil and Gas Production Sites. *Environmental*  
621 *Science and Technology*, 55(1), 581–592. <https://doi.org/10.1021/acs.est.0c06545>
- 622 Zimmerle, D., Duggan, G., Vaughn, T., Bell, C., Lute, C., Bennett, K., et al. (2022). Modeling  
623 air emissions from complex facilities at detailed temporal and spatial resolution: The  
624 Methane Emission Estimation Tool (MEET). *Science of the Total Environment*, 824.  
625 <https://doi.org/10.1016/j.scitotenv.2022.153653>

626